Zenith: DARPA's Liquid Mirror Telescope Program

Michael Nayak*[1], Denis Brousseau[4], Amanda Childers[5], Tomu Hisakado[2], Kristyn Kadala[7], Rebecca Kamire[5], Yifan Li[7], Dhanushkodi Mariappan[3], Greg Radighieri[3], Alvaro Romero-Calvo[6], Neil Rowlands[5], Paul Schroeder[2], Grey Tarkenton[7], Simon Thibault[4], Devin Vollmer[2], Santanu Basu[1] and Kaushik Iyer[1]
DARPA, North Randolph Street, Arlington, VA 22203-2114
*zenith@darpa.mil; Phone 703 526 2230

[1] Defense Advanced Research Projects Agency, Arlington, VA
[2] General Atomics, San Diego, CA
[3] General Electric, Schenectady, NY
[4] University of Laval, Quebec, Canada
[5] Honeywell, Chicago, IL
[6] Georgia Institute of Technology, Atlanta, GA
[7] Lockheed Martin, Palo Alto, CA

ABSTRACT

Astronomy and Space Domain Awareness are limited by the size of available telescope optics, the cost for which scales steeply due to the exquisitely ground and polished primary mirrors, typically made of glass or other light-weight substrates. Liquid mirrors (LMs) may break this unfavorable cost scaling. When rotated at a constant angular velocity, it has been shown that fluid surfaces take the form of a paraboloid, which can function as a primary mirror. However, current LMs cannot slew or tilt off-zenith due to gravity, greatly limiting the viewing area in the sky. To overcome these limitations while also enabling low-cost, very-large-aperture telescopes, DARPA launched the *Zenith* program. Zenith is developing entirely new LM design-for-build approaches that can create large optical surfaces and maintain optical quality during tilt and slew by correcting transient liquid surface aberrations in real time. The development of these new designs is being supported by multi-physics models, materials, surface and field controls, and structures. This paper discusses key and fundamental aspects of four new design and modeling approaches for this new class of LMs. The software and simulation tools developed by the Zenith program to design tiltable and size-scalable liquid mirrors are also available to the astronomical community as an open-source repository.

Keywords: Zenith Program, DARPA, Liquid Mirror (LM), Liquid Mirror Telescope (LMT), Tilt, Tip, Slew, Gravity, Non-Rotating, Scalable, Space, Object Tracking, Astronomy, Space Domain Awareness

1. INTRODUCTION

In the quest to map the universe, Hubble Space Telescope[1] and James Webb Space Telescope (JWST)[2] represent historic inflection points in Deep Space Observation technology owing to their size and unprecedented manufacturing precision at scale. HST has a 2.4-meter (m) diameter circular, monolithic mirror made from glass coated with aluminum and magnesium fluoride; JWST has a 6.6 m hexagonal, 18-segment mirror made from beryllium coated with gold[1]. JWST's 25 m^2 collection area allows detection of faint infrared light of galaxies 13 billion light-years away. The flatness precision required to achieve this imaging capability is equivalent to a hexagonal mirror scaled to the size of the United States with its highest peak no taller than 2 inches[3]. The science return of JWST[4] has the astronomical community looking to leverage this remarkable technological feat to build even larger telescopes in the coming decade by incrementally advancing the traditional mirror fabrication paradigm. Larger apertures serve not just the scientific community; Space Domain Awareness (SDA) in geostationary orbits (GEO) is currently choked by insufficient imaging resolution limited by the telescope mirror size as shown in Figure 1[5].

Advances in Optical and Mechanical Technologies for Telescopes and Instrumentation VI,
edited by Ramón Navarro, Ralf Jedamzik, Proc. of SPIE Vol. 13100, 1310037

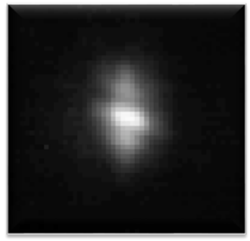

Figure 1. Image of GEO satellite GE-23 from the second largest optical telescope on Earth (10 m Keck II, with adaptive optics)[5]. Despite the large imaging aperture, the satellite is still unresolved, revealing the limitation of aperture size forSpace Domain Awareness.

Traditional Very Large Telescope (VLT) design is cost-prohibitive for apertures greater than 10 m; significant resources are needed for building, polishing and metrology for mirrors, as well as expensive adaptive optics. As space-based telescopes become larger and more costly, they also face heightened operational risk from damage by collisions with micrometeoroids and orbital debris (MMOD)[6,7,8,9]. In recognition of these obstacles to future scalability, investigation of different approaches that allow faster construction of larger and lower-cost telescopes, assembled either on the ground or in space, has commenced[10]. Diffractive lenses[11] and fluidic telescopes[12,13] are two such alternative approaches.

When rotated at a constant angular velocity about a vertical rotation axis, the equipotential surface of a fluid takes the form of a paraboloid. This is the principle behind present-day liquid mirror telescopes (LMTs): light incident upon a reflective liquid surface spinning at a constant angular velocity converges at an effective prime focal point. Cabanac et al[14] demonstrated a 3 m diffraction-limited spinning LMT made of mercury for orbital debris observations. The cost of a liquid mirror is estimated to be two orders of magnitude less than a glass mirror[15]. For example, the cost of the 4-m diameter International Liquid Mirror Telescope is ~$2 million[16], whereas the estimated cost of a 4-m conventional telescope is estimated to be >$376 million[17].

Laird et al[18] first showed that combining a ferrofluid shaped by a magnetic field with a surface-deposited metal liquid-like film (MELLF) made from a silver colloid could be used to build a deformable LM. Brousseau et al[15,19] demonstrated a residual root mean squared wavefront error less than 0.05 μm with a ferrofluidic deformable mirror shaped by an array of 91 ~3 mm-diameter magnetic cores placed beneath the liquid, and a superimposed larger steady circumferential magnetic field generated by a Maxwell coil. The 4-m diameter International Liquid Mirror Telescope (ILMT) in Davasthal, India saw first light in April 2022[20]. The mirror spins at 7.5 rpm to create a parabolic mirror shape. Limited by gravity, the liquid mirror has a field of view of 0.36 deg around zenith.

Despite this progress, fundamental limitations such as not being able to tilt remain with traditional LMTs, which has limited their utility to the astronomical and space domain awareness communities. Traditional LMTs can only point straight upward (zenith-restricted) and are, therefore, limited to isotropic sky surveys. Any application of tip or tilt results in the liquid sloshing out and the imaging capability of the telescope being lost. The need for spin-rotation or thrust-for-gravity to form a coherent liquid mirror surface also restrict space deployment of LMTs. Due to the necessity for spin, segmented mirrors, which are the standard for large space-based telescopes, are not possible with LMTs.

Recent work has opened new paths for potentially implementing tiltable liquid mirrors. Wang et al[21] investigated ferrofluid infused microporous surfaces subjected to a magnetic field, and demonstrated combined magnetic and capillary actuation and control of a ferrofluid through an engineered capillary microchannel, and more complex flow paths. They also showed that a droplet can be magnetically forced to maintain its shape while tilting up to 90 degrees in the presence of gravity. Caillosse et al[22] showed that ultrathin adherent reflective films of homogeneously self-assembled silver nanoparticles (AgNPs) can be generated in-situ by exposing an aqueous solution containing a silver precursor and a photogenerator to UV light for a few seconds. Khan et al[23] demonstrated how interfacial tension of liquid metals can be reversibly controlled by applying voltage. Eaker and Dickey[24] investigated reversible shape changes of gallium-based LMs upon applying a voltage, and reviewed four methods of LM actuation: electrocapillarity, continuous electrowetting, electrowetting-on-dielectric (EWOD), and electrochemically controlled capillarity. EWOD does not require the LM to be immersed in an inert electrolyte, and may be scalable and easy to fabricate. Ren et al[25] demonstrated focal length control of a liquid lens using a servo motor to induce hoop compression on the convex lens and thereby induce curvature change. Li et al[26] achieved a similar result using a piezoelectric motor. Corning's Varioptic®[27] liquid lens uses an electrostatic field to control the curvature, and therefore focal length, of a liquid lens. This change is effected in ~10 ms by changing the applied voltage. In summary, these advances offer proofs-of-concept for tiltable, slewable, scalable and segmentable milimeter-scale LMs using capillary, electrostatic and magnetic forces.

The present work explores the scalability of these concepts to the meter-scale LMs and the challenges therein, built upon the research advances described above. In this paper, we report on four LM prototype development initiatives, from teams led by General Atomics (GA), General Electric (GE), Lockheed Martin (Lockheed) and Honeywell. All four efforts strive to prove the feasibility of a scalable liquid mirror. The proof-of-concept hardware development is backed by a robust modeling and simulation (M&S) effort. Under funding from the Defense Advanced Research Projects Agency (DARPA), the "Zenith" program's near term (33-month) goal is to demonstrate through hardware and M&S, a liquid mirror with the following characteristics[28]:

- Optical aperture diameter of at least 0.5 m, and a focal length in the range of 1 to 10 m.
- Liquid system that covers the entire LM aperture and that has specular reflectivity of greater than 0.65 at a reference wavelength of 550 nm,
- Out-of-plane tip and tilt angles of greater than 10 degrees,
- 0 to 1 degree/second slew rate,
- Wavefront error, correctable to a sixth of a wavelength root mean squared (RMS) error across the entire effective aperture during slew and at rest at a reference wavelength of 550 nm

The vibration environment and real-time fluid control must permit this level of wavefront error rejection, which is expected to be the pacing technical challenge. Each of the four design concepts is a new and unique build-concept for a 0.5-m aperture LM system, supported by multi-physics analysis and M&S. Successful designs may be scaled up to the 1-m and larger sizes in future phases of the program.

The need to spin traditional liquid mirrors has previously limited their scaling to VLT sizes. Instead of the liquid mirror surface scaling unfavorably in cost, the size of the required torque motor would instead scale unfavorably. In an advance to this state-of-the-art, Zenith LMT systems may not use spin.

2. APPROACHES TO A TILTABLE, SLEWABLE AND SCALABLE LMT

Figure 2 summarizes the approaches to extend the research discussed in Section 1 at the coupon scale to the 0.5 meter prototype scale and beyond.

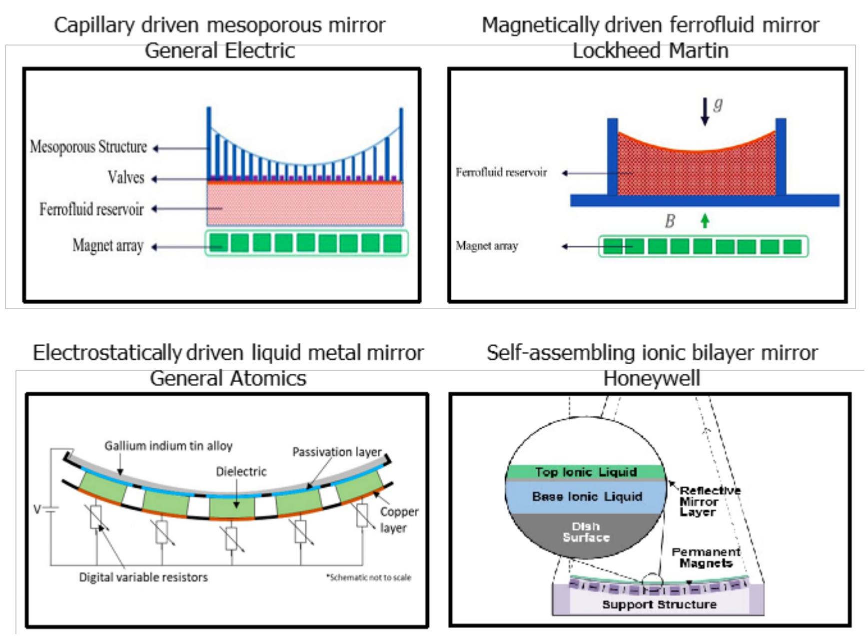

Figure 2. The DARPA Zenith program is advancing LM design-to-build 0.5-meter mirror concepts that implement magnetic, capillary, electrostatic and piezoelectric control of ferrofluids and liquid metals. Schematics are not to scale.

These four methods use a combination of reflective liquids development, mirror surface metrology and control, system-architecture development, newly developed physics-based M&S capabilities and laboratory tests. These include:

(1) A capillary actuated, electromagnetically controlled liquid surface. The lead organization is General Electric, with the University of Laval and Raytheon Technologies Research Center[29] as team members;

(2) An electromagnetically driven and controlled ferrofluid surface. The lead organization is Lockheed-Martin, with the University of Arizona[30] as a team member;

(3) An electrostatically driven and piezoelectrically controlled mirror design with a liquid metal as the optical fluid. The lead organization is General Atomics[31];

(4) The use of two immiscible ionic liquids controlled primarily by permanent magnets. The lead organization is Honeywell, with Georgia Institute of Technology and Soter Technology[32] as team members.

All methods seek to base the formation of an imaging surface and shape on field control of a working liquid, without the use of rotation or thrust, for the first time. Approaches (1), (2) and (4) investigate the scaling of these concepts both experimentally and using new simulation tools, with reflective ferrofluids or bilayer ionic liquids. Approach (3) investigates the feasibility of scaling up the EWOD behavior shown[23,24] by a non-reflective Gallium-Indium-Tin (GIT) liquid alloy at the droplet level, to a half-meter scale LM, using experiments and newly developed simulation tools, and mercury as the working fluid.

The following subsections summarize each of these methods, and work accomplished to date.

2.1 Mercury Liquid Mirror Based on Electrowetting-on-Dielectric (EWOD) Approach

This approach is an electrostatically driven and piezoelectrically tuned segmented LM system, with a mirror diameter of 50 cm. The liquid metal chosen for this design is mercury, which is conductive, but also has LMT heritage from previous work on the NASA Orbital Debris Observatory[14]. Figure 3 shows a schematic of the concept. Additional details may be found in reference 31.

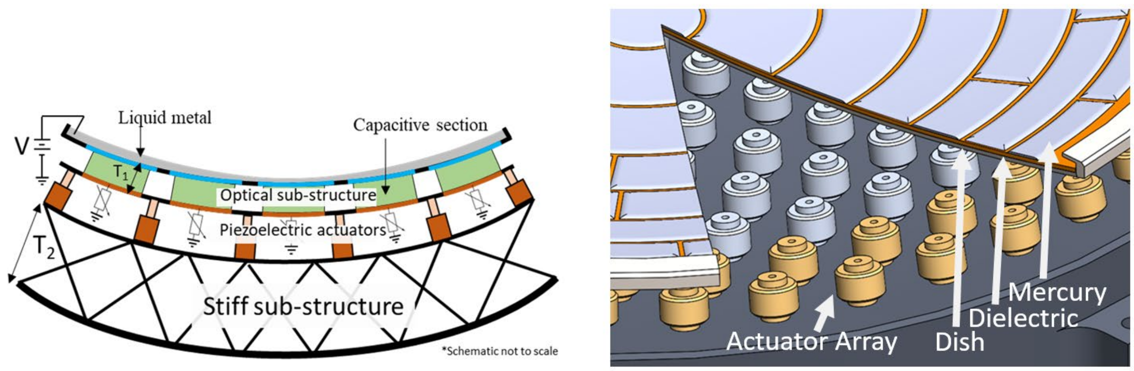

(a) (b)

Figure 3. The liquid mirror design based on the EWOD approach. (a) schematic showing the key sub-systems of the liquid metal-based mirror and a conceptual implementation in a telescope, and (b) CAD drawing showing mirror segmentation, paraboloid dish and piezoelectric actuator array used for fine control of the mirror surface. Figures courtesy General Atomics.

The mirror substrate is a curved (paraboloid) dish to match the required mirror curvature. The substrate is coated with a dielectric material to aid in spreading of mercury and the adhesion of mercury to the substrate. The design relies on the EWOD principle, i.e., the ability of a thin film of mercury to spread when voltage is applied at the top surface of the mercury layer, and the bottom of the substrate is grounded. The design compels the top surface of the mercury to assume the desired mirror shape before correction by uniformly spreading due to EWOD effect, and by conforming to the curved shape of the substrate.

The mirror design is segmented as shown in Figure 3. The segment size is determined by the largest mercury mirror that can be made by the EWOD principle. The substrate is supported on a stiff sub-structure with an intermediate actuator layer, as shown in Figure 3(b). During slew and at rest, the mercury surface in each segment needs to create a high optical quality surface and conform to the curvature prescription. All the segments need to be maintained in phase during operation to enable diffraction-limited imaging by the entire mirror aperture. This is to be accomplished by a combination of global and local actuators, and by a combination of piezoelectric and DC-motor-driven actuators in the actuator layer. Closed loop wavefront error control of the mercury mirror surface will be implemented using a wavefront sensor and the suite of actuators.

To investigate electrostatic field strengths, adhesion to the substrate and other conditions necessary for achieving a stable contiguous Mercury film on a dielectric substrate, a custom test apparatus with a built-in glove box and fume hood has been built (Figure 4). This experimental setup safely supplies high electric fields while the mirror substrate is tilted up to 10 degrees along two axes. Initial experiments are focusing on flat dielectric substrates and substrates in the form of a container. Testing with this set-up is ongoing. The competing requirements of liquid spreading and adhesion crucially depend on the properties of the dielectric layer between the mercury and the substrate.

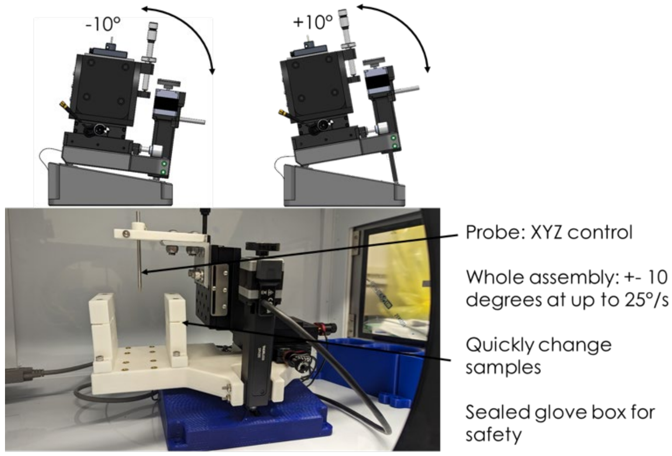

Figure 4. Test apparatus for investigating electrostatic wetting on dielectric (EWOD) effects to create a large-area mercury mirror.

To develop a baseline mirror design, multi-physics simulation of mercury spreading on a dielectric substrate is in progress, using analytical models and COMSOL. Models include the effects of gravity, liquid viscosity, liquid surface energy and interfacial friction, in addition to coupling electrostatics with the fluid mechanical response. Most simulations were performed in 2D; full 3D simulations have long computational run times. Eventually, 3D simulations will be required to model tilting and slewing.

Figure 5 shows one example of results from a mercury spreading simulation. In this example, the profile of a mercury droplet is shown in half (symmetric) at 0.5 s after application of voltage between the droplet and the substrate, with a layer of dielectric in between. The results show that a mercury droplet with a size (radius) of 2.5 mm at zero voltage expands to 5.8 mm under 800 V of applied voltage. Simulations are in progress to compute the profile when the substrate is tilted from 0 to 10 degrees.

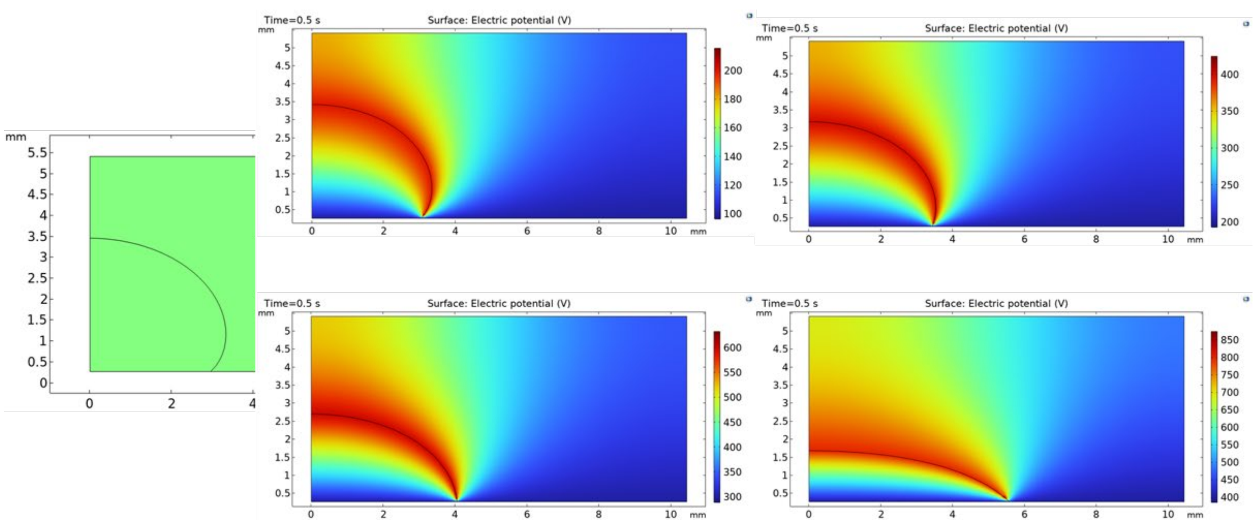

Figure 5. Representative COMSOL simulation of the electrostatically induced mercury droplet profile versus applied voltage. The profiles are shown 0.5 s after the voltage is applied and when steady state is reached.

Simulations of the piezoelectric actuator array to control the substrate shape of the half-meter diameter LM are being performed, using ANSYS and ZEMAX. Given actuator properties such as stiffness and tip size, the number of actuators, the substrate material and thickness, deformations of the substrate can be calculated. Simulation results are then used to optimize the actuator subsystem. The ANSYS mechanical analysis provides the substrate profile and sag between actuators. The dish surface shape from ANSYS is used as input to ZEMAX, which performs the optical wavefront error computation for the substrate.

A typical simulation output showing deformation and wavefront error of the substrate is shown in Figure 6. For these results, the substrate is assumed to be of optical quality.

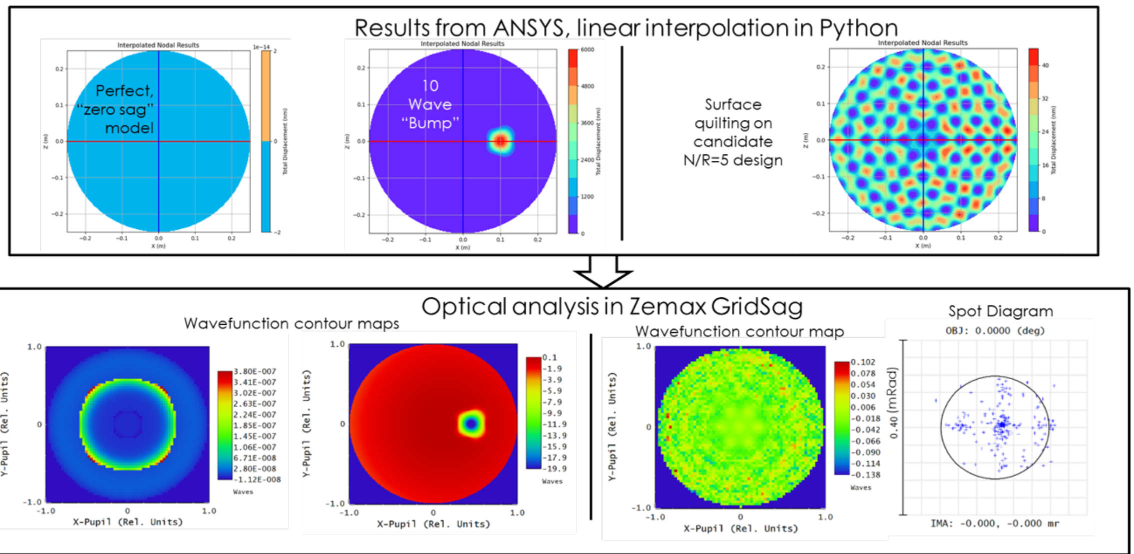

Figure 6. Modeling flow that takes ANSYS deformation/sag output and provides it to ZEMAX, which computes wavefront error.

Prior work in the literature on EWOD modeling of mercury was limited to millimeter (mm) scale droplets. One of the accomplishments of this effort has been the development and expansion of a mercury spreading and adhesion model to centimeter (cm) scale. The modeling tools may be applied to liquid metals other than mercury. The code base developed by the GA team is discussed in Section 3.

2.2 Capillary-Assisted and Magnetically Controlled Ferrofluidic Approach

This approach is a capillary-force assisted, and magnetically controlled LM system, with a mirror diameter of 50 cm. The liquid chosen for this design is a two-component liquid system, typically 2-5 mm thick, comprising a ferrofluidic layer with a top reflective layer. Ferrofluids are made of a suspension of magnetic nanoparticles in a suitable solvent. Ferrofluids have very low reflectivity in visible wavelengths. To form a mirror, a metal-like liquid film (MELLF) layer containing silver nanoparticles and organic ligands is applied to the top of the ferrofluid layer[15]. The MELLF combines the property of high reflectivity of silver and liquid-like behavior that allows it to form a thin uniform layer on the ferrofluid surface that can be controlled by magnetic field. Figure 7 shows a schematic of the concept. Additional details may be found in reference 29.

This approach is being investigated by a team from General Electric, with the University of Laval. The magnetically-controlled ferrofluid development builds on work done by Brousseau et al[18,19], which demonstrated a 23-mm optical aperture ferrofluidic deformable mirror.

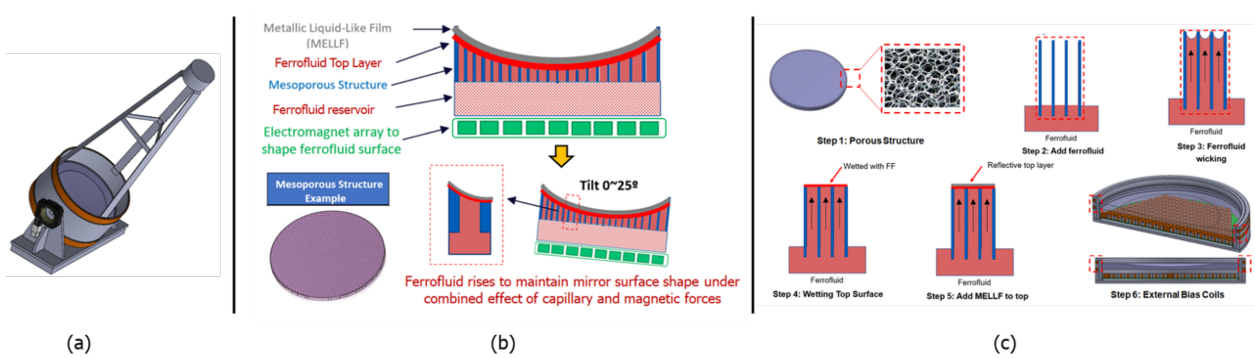

Figure 7. Schematic of a capillary-assisted magnetically controlled ferrofluidic mirror and telescope.

Figure 7(a) shows a first design of a liquid mirror telescope with wavefront error diagnostics. Figure 7(b) and 7(c) show the design schematic for the capillary-assisted magnetically controlled ferrofluidic mirror. A paraboloid mesoporous dish provides the basic mirror shape to the liquid surface, which is then controlled by a magnetic sub-system consisting of an underlying electromagnetic coil array and circumferential Helmholtz coils. The Helmholtz coils simplify the liquid surface response function. The deformation at the liquid surface increases with the applied magnetic field. When the magnetic field exceeds a critical value (typically 80 Gauss in some cases[15]; for comparison, the Earth's magnetic field is less than 0.67 gauss), spikes appear on the liquid surface. The design ensures the magnetic field remains below this so-called Rosensweig instability limit[33].

Capillaries serve two purposes – dampening the fluid motion during tilt and slew and delaying formation of the Rosensweig instability. Submerged in the ferrofluidic layer is a capillary ("mesoporous") structure which combines capillary forces with magnetohydrodynamic forces to control the optical surface of the MELLF layer in presence of tilt and slew. The typical pore size is 50-micron in diameter. Figure 7(c) shows the curved substrate for the ferrofluid mirror and the bias coils of the electromagnets underneath. The ferrofluid rises through the capillaries and a reflective MELLF layer is formed on top of the ferrofluid surface above the capillaries. Two types of capillary structures are being investigated: structures with random-sized pores (foam) and structures with uniform sized (machined) holes. Different material classes for the capillary substrate and the height and diameter of the capillary channels, are being actively optimized for the liquid mirror application.

The liquid system developed by GE is a custom ferrofluid with a submerged porous structure (which aids in controlling the liquid mirror surface) and a custom MELLF layer which gives more than 65% reflectivity. Figure 8 shows the picture of the liquid surface and a wavefront error map of the surface at rest showing $\lambda/7$ rms uncorrected wavefront error measured at 633 nm[29]while at rest.

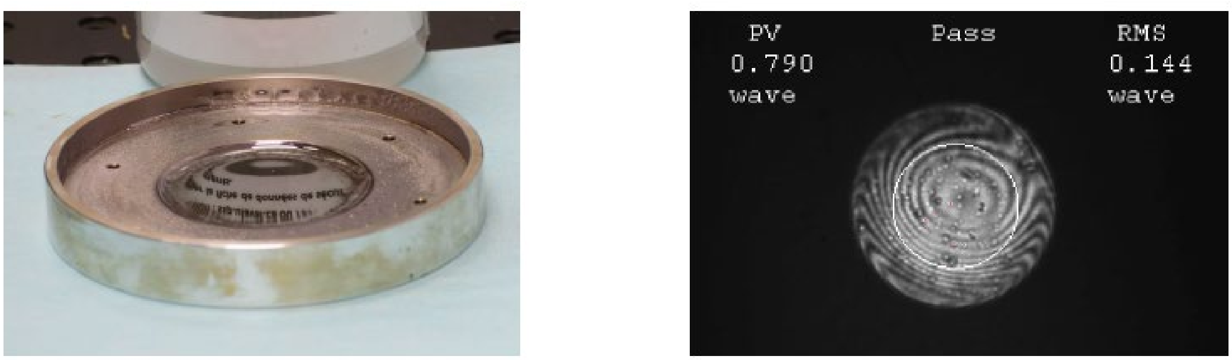

Figure 8. The GE liquid mirror with ferrofluid and MELLF[29] (left) and measured surface wavefront quality while at rest (right).

The ferrofluid shape is controlled by an electromagnet subsystem, which consists of an underlying electromagnetic (EM) coil array and two Helmholtz coils, shown in Figure 9. The Helmholtz coils produce a strong and uniform magnetic field throughout the ferrofluid. An array of electromagnets under the mirror substrate carry out fine control of the ferrofluid surface shape, working in the linear regime of magnetic field versus current. The major advantage of this linearization is that one can use the same proven algorithms that are used with solid deformable mirrors. The magnetic field of the Helmholtz coils is at least 10x larger than the magnetic field from a single EM coil, which indicates that the design is within a linear regime. The surface response, linearized with a strong and uniform magnetic field from the Helmholtz coil, can be 50-100x the field strength generated by a single EM coil.

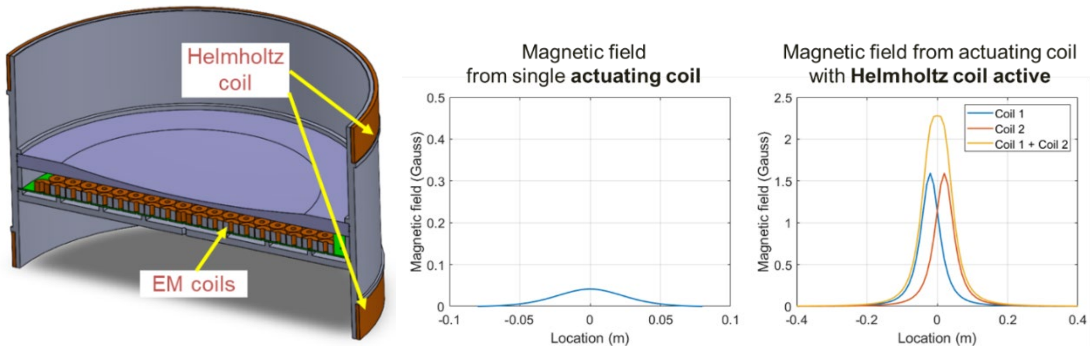

Figure 9. Modeling of representative designs combining Helmholtz and EM coil arrays ensures that the mirror surface response is in the desired linear regime.

The response of the ferrofluid surface for different coil arrangements have been modeled to optimize the magnet sub-assembly. COMSOL simulations have been verified against analytical solutions (see Section 3). Figure 10 shows the influence function of an electromagnet on the ferrofluid surface calculated both analytically and with COMSOL, showing good agreement between the two. Modeling of the field generated by the magnets have yielded an optimized number of electromagnet coils. Power dissipation from the Helmholtz coils has been found to be small and insensitive to the wire gage used for the 50-cm mirror design.

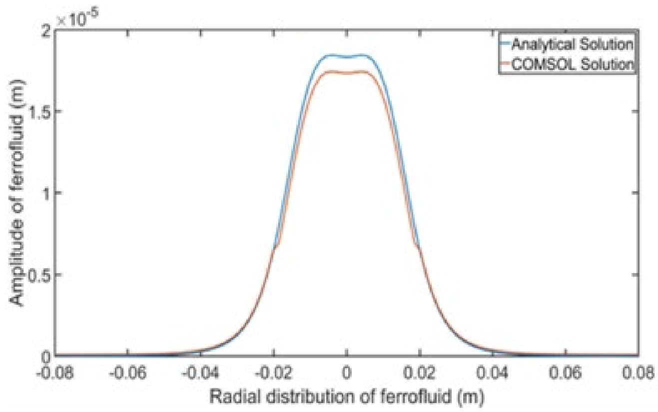

Figure 10. Comparison between analytical modeling and COMSOL simulations.

A full suite of analytical models are being developed for this LM approach. This includes (1) magnetic field modeling, (2) magnetohydrodynamic modeling, (3) fluid dynamics modeling including gravity, capillary effect and physical motion of the mirror, and (4) controls system modeling.

2.3 Magnetically Controlled Ferrofluidic with a Porous Wicking Structure Approach

This approach, led by Lockheed Martin, is a magnetically controlled ferrofluidic liquid system for a liquid mirror diameter of 50 cm. The liquid system chosen for this design is a commercially available ferrofluid, which gives the surface shape, and a custom MELLF layer on top, which gives the desired reflectivity. The MELLF contains gold nanoparticles to give high reflectivity for visible wavelengths. A porous wicking structure submerged in the liquid to give additional control of the surface layer against gravity is an option. Figure 11 shows a schematic of the concept. Additional details may be found in reference 30.

A fluid reservoir with a liquid retention film at the bottom contains the ferrofluid. The liquid-retention substrate is curved to match the desired mirror prescription. A magnet subsystem containing an array of electromagnets is positioned underneath the ferrofluid layer to control shape and achieve wavefront error correction of the fluid surface. A porous wicking structure submerged in the ferrofluid, as shown in Figure 11, is an option being actively traded. The role of the capillary wicking structure is to reduce required fluid volume, increase liquid surface stability, and increase liquid surface area scalability. Preliminary modeling results suggest that the wicking structure may not be needed in a 50-cm diameter mirror design. The ferrofluid extends above the wicking structure. The shape and the figure of the liquid are maintained by a combination of the magnetic force (from the magnet subsystem), surface adhesion force, and optional capillary force.

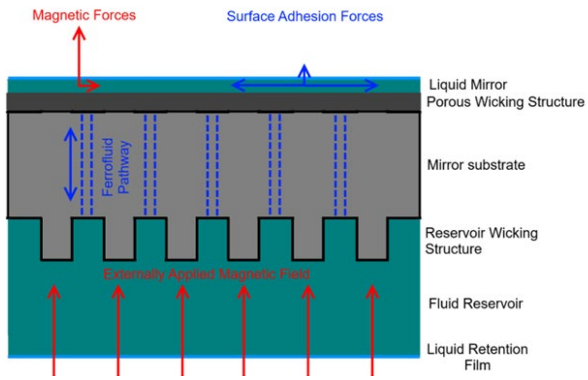

Figure 11. Schematic of the magnetically-controlled ferrofluidic with a porous wicking structure approach.

After carrying out trade studies for the liquid system, a commercial ferrofluid with low vapor pressure and high viscosity has been chosen. For the MELLF layer, experiments were carried out using silver and gold nanoparticles of various sizes, shapes and concentrations. Ligands were optimized to make the MELLF compatible with the ferrofluid and to increase the lifetime of the liquid system. Application process of the MELLF on top of the ferrofluid layer was optimized. As a result, a sub-scale reflective liquid system that can be controlled by a magnetic field was developed.

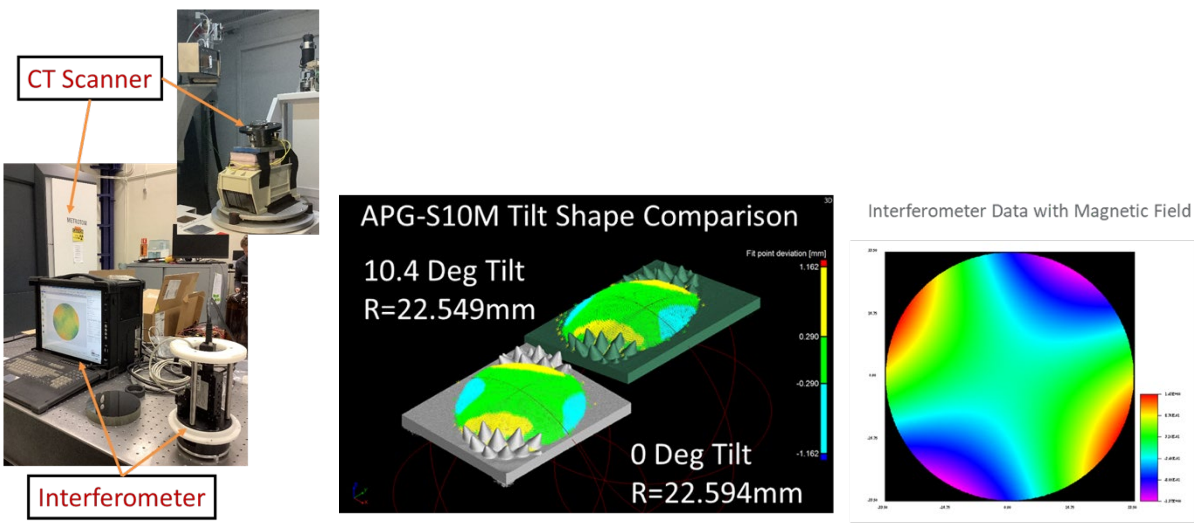

(a) (b) (c)

Figure 12. (a) Experimental set up to investigate applicability of interferometry, X-ray Computed Tomography, and a Keyence Microscope, to characterize the shape and smoothness of LM surfaces, (b) demonstration of ferrofluid curvature maintenance at 10 degree tilt while under the control of a permanent magnet. Onset of the Rosensweig instability at two regions is also imaged, and (c) interferometric data obtained in the upright (no tilt) position.

Experiments were conducted to study the physical and optical characteristics of ferrofluids in magnetic and gravitational fields. The experimental set up is shown in Figure 12. A sample holder was designed to hold the ferrofluid and a permanent magnet. The sample holder is tilted using optical stages. The surface profiles are measured using interferometry and X-ray computed tomography (CT scan). The interferometer had a field of view of 494 µm x 494 µm. As shown in Figure 12, the shape of the ferrofluid sample and the surface roughness did not change appreciably when the sample holder was tilted between 0 and 10 degrees. The CT scan showed surface perturbations due to Rosenzweig instability at two edges of the ferrofluid sample. Figure 13 shows the measured ferrofluid surface roughness values in the 2-5 nm rms range at applied magnetic field strength values between 0 and 250 G.

Preliminary measurements indicate a surface roughness less than 5 nm RMS within this field of view in presence of a magnet. As shown in Figure 13, the shape of the ferrofluid sample and the surface roughness did not change appreciably when the sample holder was tilted between 0 and 10 degrees.

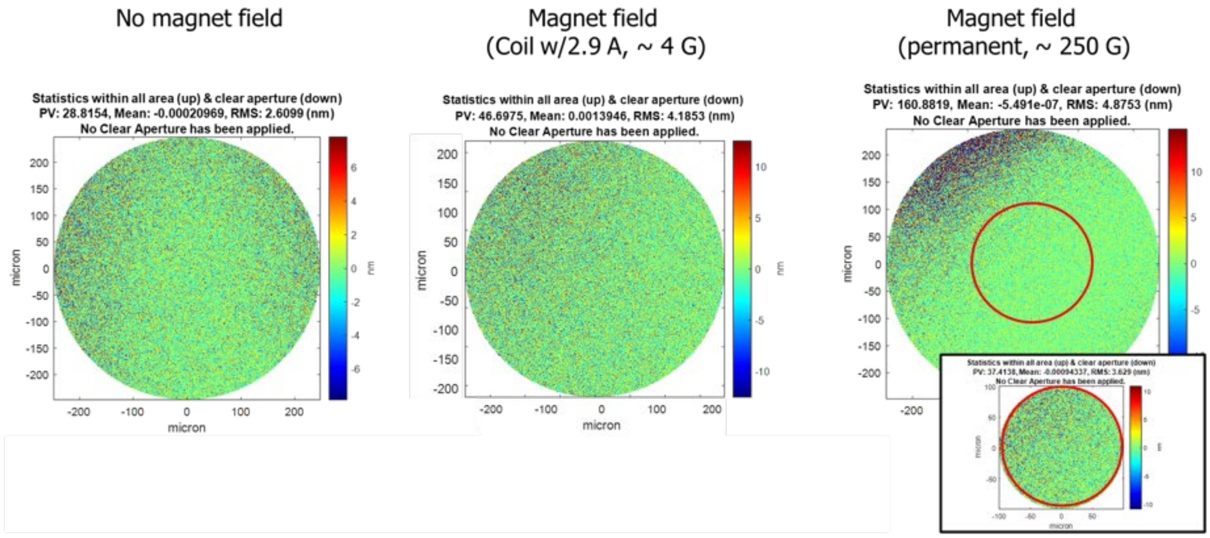

Figure 13. Interferometric surface roughness measurements as a function of magnetic field strength.

In the M&S effort, magnetic field profiles in the ferrofluid have been calculated for linear coils. The ferrofluid surface profile has also been calculated using an arrangement of coils to impart the desired shape. For linear coils, the field is mostly parallel to the coil axis and is maximum at the ends. Basic model predictions aligned well with test data from the small-scale experiment described above. The equations for surface shape function have been analytically derived (see Section 3)[30]. An effort is under way to incorporate the analytical model into finite element simulations.

2.4 Magnetically Controlled Self-Assembling Ferrofluidic Ionic Bilayer Liquid Approach

This approach is a magnetically controlled self-assembling ferrofluidic LM system that uses an ionic bilayer liquid structure, with a mirror diameter of 50 cm. The liquid system comprises a base ionic liquid that contains magnetic particles and is ferrofluidic, a liquid with reflective nanoparticles, and a second ionic liquid that caps the reflective layer and serves as the optical surface of the mirror. Figure 14 shows a schematic of the concept. Additional details may be found in reference 32.

The mirror surface shape and optical quality of this LM system are controlled by a combination of permanent magnets and electromagnets. A key feature of the concept is its self-assembling nature. This ferrofluidic ionic liquid mirror telescope constructed from two immiscible ionic liquids containing spatially segregated reflective and magnetic nanoparticles, positioned by a Halbach array of permanent magnets. The substrate is curved to match the optical prescription of the primary mirror. When the base ionic liquid, the reflective nanoparticle liquid layer, and the optical surface ionic liquids are mixed and allowed to settle, the ionic layers separate out and the reflective layer is sandwiched between the two ionic layers. The top layer of the substrate also plays a role in spreading and retaining the liquid system.

Processes to prepare magnetic particles for suspension in ionic liquids, as well to produce the reflective layer have been developed and tested experimentally at the small-scale. Experiments have been conducted to study the spreading behavior of ionic liquids on various substrates. The reflectivity of test reflective layers on ferrofluid has been measured for several design choices. Progress has also been made towards developing commercially sourced ionic liquid pairs with reflectivity in excess of 65% at 550 nm. Figure 14 shows a diagnostic set up in which the reflected light from the mirror is focused and analyzed at the focal plane of a telescope.

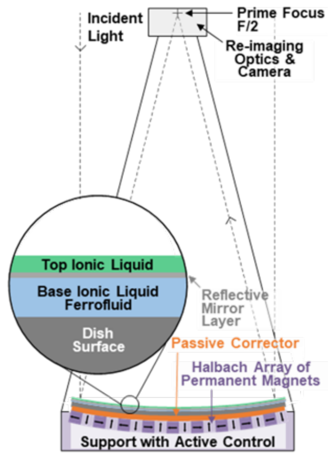

Figure 14. Schematic of a Self-assembling Ferrofluidic Ionic Liquid Mirror Telescope.

The primary figure control of the ionic ferrofluid is done with a Halbach array. The Halbach array creates a magnetic equipotential surface away from the array and parallel to the top plane of the array. Preliminary ferromagnetic modeling led to the design and construction of a 10”x10” Halbach array prototype with 400 half-inch cubic magnets, shown in Figure 15. The magnets were commercially procured and measurements showed only 2.5% maximum variability in the magnetic flux density across the lot. The test showed that the assembly requires controlling deformations within the array due to strong magnetic forces in the vertical direction. The fabricated Halbach array demonstrated the ability to hold a ferrofluid and its surface at a tilt angle of 90 degrees also shown in Figure 15. The figure shows that a beaker containing a commercial ferrofluid is held horizontally against gravity by the Halbach array and the fluid continuity is maintained by the magnet.

To investigate and validate the influence of as-built Halbach arrays on LM surface quality, and other test conditions that cannot be easily captured by modeling, a custom test apparatus with an interferometric system was built (Figure 16). The set-up characterizes mirror wavefront error while tilting greater than 10 degrees. It uses a circular optical bench with a steel baseplate in its center for placing and positioning a glass beaker containing a liquid mirror sample (Figure 15). A Halbach array can be positioned precisely underneath an LM sample, exploring the influence of distance (and field strength) on mid-frequency wavefront error, and on global wavefront error under tilt. Tests are ongoing to understand design implementation issues, and to anchor experimental results in M&S.

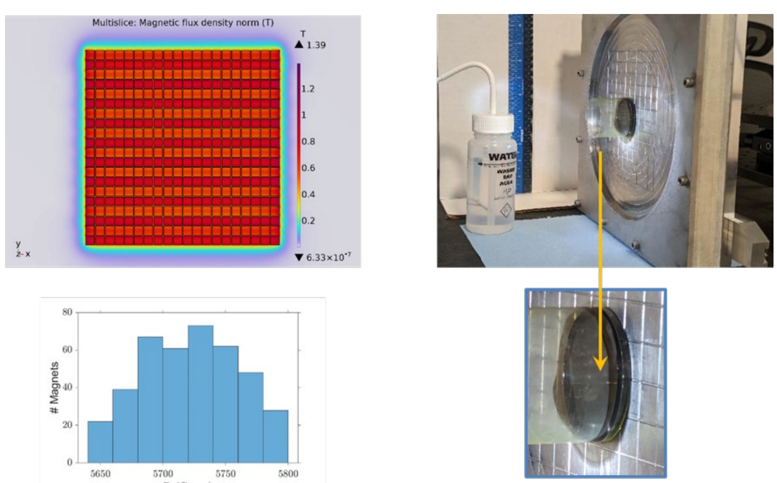

Figure 15. Assembled Halbach array (top left), statistics of magnetic induction of commercially procured magnets (bottom left), a beaker containing ferrofluid held horizontally with a vertically oriented Halbach array (top right), and an enlarged view of the magnetic fluid at 90-degree tilt angle to the vertical (bottom right).

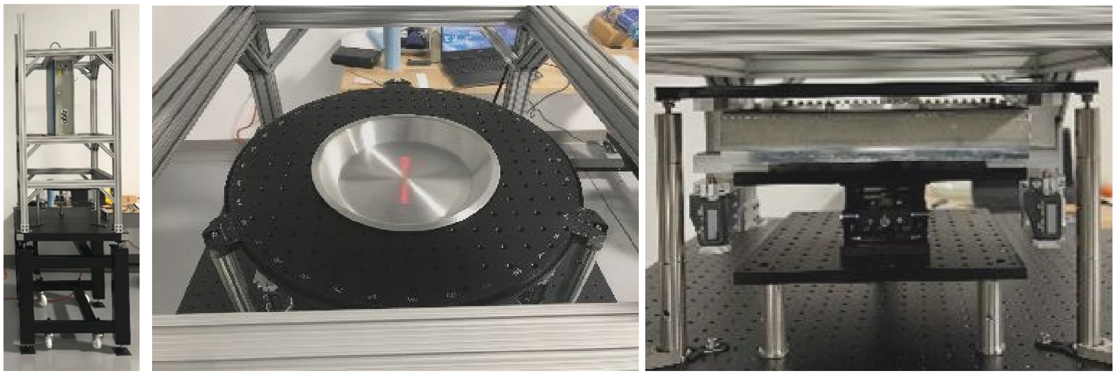

Figure 16. Interferometric test set up to measure the optical quality of the ionic liquid-based mirror.

The Halbach array shown was designed using a custom model. Figure 17 shows the computed Kelvin body force magnitude and magnetic field from an array of 400 magnets. This model was also used to estimate the mid-frequency WFE induced in the LM, which is then used to design tailored magnetic shims added on top of the Halbach array to further reduce magnetic field variations and enhance magnetic control.

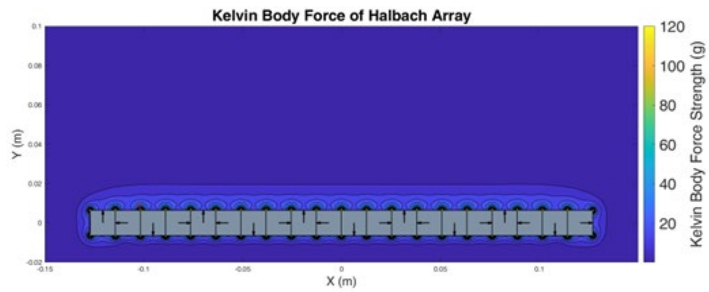

Figure 17. COMSOL simulation of a linear Halbach array of permanent magnets generating a flat magnetic force field on a ferrofluid layer.

Both analytical and finite element models have been developed to predict ferrofluidic behavior and optical surface aberration in presence of gravity. Simulation results have shown that tilting off-axis requires active control or compensation. A separate 2D analytical model, that integrates a model of a Halbach array and ferrofluid and COMSOL, showed that the Halbach array magnet size impacts global and mid-frequency wavefront error (WFE) in opposite directions, i.e., global WFE (from tilt) are minimized by large magnets while mid-frequency WFE (from array periodicity) is minimized by small magnets. A key finding is that mid-frequency WFE is independent of tilt, and so global and mid-frequency WFE can be controlled separately. Representative results from physics-based modeling are shown in Figure 18.

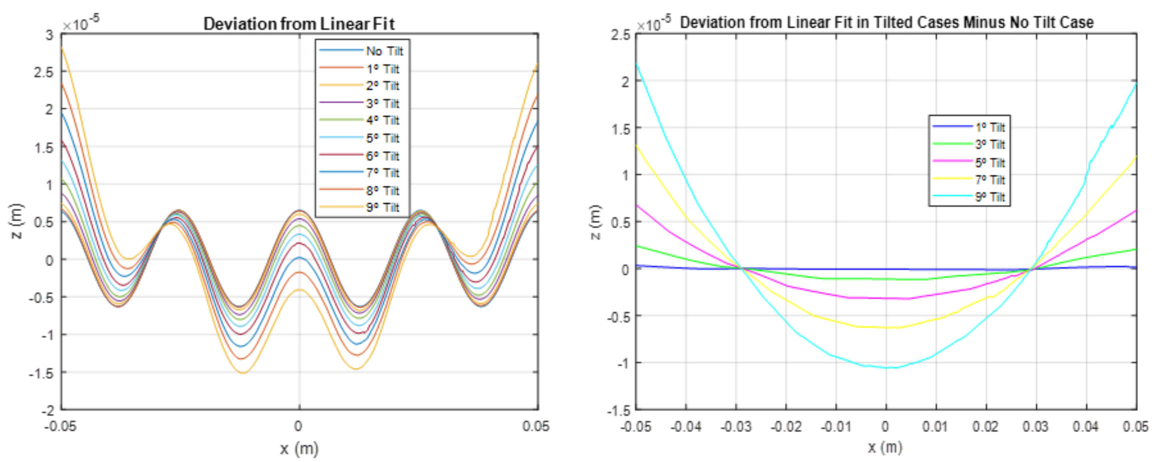

(a) (b)

Figure 18. Representative results from physics-based modeling: (a) sum of global and mid-frequency WFE for different tilt angles, (b) leaves only global WFE only, after subtraction of mid-frequency WFE for no tilt.

Early identification of key design trades was achieved through an analytical approach, followed by finite element analysis simulations to evaluate complex scenarios. This analysis showed that smaller magnet wavelengths favor surface ripple control but increase errors when tilting. Larger magnet wavelengths are better not only for tilting control but are also easier to manufacture. The team has identified a need for active control to effectively mitigate excess surface ripples, and design iterations are ongoing. The code base developed by the Honeywell team is discussed in Section 3.

3. AVAILABILITY OF LIQUID MIRROR MODELING CODE

An important part of the Zenith program vision was to create the capability for the broader astronomy community to investigate, validate, build, and proliferate tiltable liquid mirror telescopes for civil and commercial use. Since the utility of current liquid mirror telescopes is limited by the small viewing area at zenith, tiltable Zenith liquid mirror telescopes may greatly enhance the utility of LMTs in general, while offering significant cost benefits over traditional glass optics at large aperture sizes. The simulation tools developed to validate these designs may be useful to the astronomy community for designing future liquid mirror applications.

All four Zenith teams have developed open-source coding tools, together with in-code comments and instructions for use. This section describes those code bases, and instructions for accessing them.

3.1 General Atomics Code base

The code base and documentation developed by General Atomics[31] contains a M&S documentation file and the computer code bases in four areas: (1) physics modeling, (2) mechanical modeling, (3) controls system modeling and (4) fundamental modeling. The M&S documentation file contains the physical properties of the LM components and design variables, and describes in detail the analytical framework and the underlying physics . The analysis is applicable to liquid metals other than mercury as well. It also provides an overview of all four code bases and detailed operating instructions.

In this code base, fluid dynamics is combined with electrostatics in COMSOL multiphysics. The modules used for the simulation are computational fluid dynamics laminar flow, mercury/air interface, electrowetting and electrostatics. Evolution of the liquid mercury surface on a curved surface is simulated under gravity load environment using a basic electrowetting model with surface tension, viscosity, and coefficient of friction as parameters. The original goal was to model a monolithic 50-cm diameter curved mercury surface held in place by electrostatic forces. However, the model did not converge even after running for a long time. An alternate segmented aperture design was developed with small containers of mercury forming segments of a 50-cm diameter curved mirror. This design can be simulated using an electrowetting model and under various slewing conditions. Residual uncorrected surface form error of +/- 50 μm was observed for a multi-container configuration over a 45 mm radius. The ANSYS model carries out deformation analysis of the mirror substrate under gravity load and in the presence of piezoelectric actuators which are used for shape control. The controls simulation provides voltages to be applied to the piezoelectric actuators for substrate shape control. Finally, the fundamental modeling codes provide contact angles and voltages necessary for wetting various dielectric layers between mercury and the grounded substrate.

3.2 General Electric Code base

The code base and documentation developed by the General Electric team[29] contains a M&S documentation file and the computer code bases in three areas: (1) analytical models, (2) COMSOL Multiphysics models, and (3) controls models. The M&S documentation file contains the physical properties of the liquid mirror components and the design variables, and it describes in detail the analytical framework and the underlying physics.

The analytical models compute influence function for single coils, magnetic field generated by Helmholtz coils and electromagnetic coils, 1D and 2D simulation of influence of coil design parameters and magnetic field calculation of a tilted coil.

The 2D COMSOL model includes simulation of ferrofluids interacting with porous media and Helmholtz and electromagnetic coils. In the numerical model, the LM consists of three layers: a reservoir (ferrofluid) layer, a capillary (porous) layer and the top surface of the ferrofluid layer. It is assumed that the reflective MELLF layer with any protective layer on top conforms to the ferrofluid surface and does not impart any additional surface deformation. The ferrofluid in the reservoir rises up in the porous media due to the capillary force and extends above the capillary structure to form a top surface layer. The magnetic field is calculated for the given magnet array design. The magnetic force term in the ferrofluid is computed. The magnetic force term along with gravity are included in the Navier-Stokes equation for fluid flow. Laminar condition is approximated due to low velocity of the ferrofluid under nominal operating conditions.

To model the porous media and the top layer, Darcy's Law is applied in conjunction with the phase transport equation, as the fluid flow represents a two-phase flow consisting of air and ferrofluid. Darcy's Law is coupled with the phase transport equation by setting the mass source term in Darcy's Law equal to the sum of the mass source terms for each individual volume fraction. The inputs to the model include ferrofluid properties, operating current for the magnets, geometrical parameters of the design, porous media properties and gravity. Porous media properties are added to the COMSOL code. Capillary and Bond numbers are then calculated. The 2D model shows time dependent flow of ferrofluid through the porous media, and are checked against analytical results. 2D analysis for magnetic field calculation was extended to a 3D COMSOL code. Time dependent top surface profile results can be obtained for various slewing conditions. Work is ongoing to check the simulation results against laboratory tests and to generate more accurate surface deformation results by employing finer grid sizes.

The controls model computes surface deformation at various locations in the mirror due to applied current at a single electromagnetic coil. This analytical model computes the cumulative deformation of the LM surface using superposition of transfer functions due to all EM coils. For the controls model in this version of the code, a unit cell is defined as consisting of ferrofluid without a porous structure and an electromagnet actuator. The Matlab code produces Bode plots and Step response plots of the unit cell's dynamic operation. The bandwidth of the unit cell for step function input can be computed for open and closed loop operations.

3.3 Lockheed Martin Code base

The Lockheed Martin code base and documentation[30] contains an M&S documentation file and code that can be used to study magnetic field for various coil magnet designs. The documentation file describes the analytical framework for the liquid mirror system, including the calculation of magnetic field for various magnet geometries, the response of the ferrofluid to the magnetic field, and simplified code optimization by order of magnitude calculations of effects such as surface tension and viscous damping.

The Matlab code calculates the magnetic field using Maxwell equations for a magnet arrangement. Given the magnetic field, it calculates the magnetic force on the ferrofluid.

The documentation presents the equations to be solved for the mirror design, and points out computational difficulties in solving them. The difficulties arise primarily due to the large aspect ratio of the fluid bed (diameter to thickness), the fluid to air boundary determined by nonlinear differential equations, mirror dynamics, and the need to determine the liquid surface location to ~1/40th-wavelength accuracy, whereas the liquid thickness is few thousand times the wavelength. This creates a challenging setup.

Several useful observations are made to guide future modeling development. The first is that creeping (or Stokes) flow can be assumed. Considering the surface tension force, it was concluded that surface deformations less than 1.75 mm in lateral scale would be smoothed out. In this design, Rosensweig instability is predicted to occur at a much lower magnetic field than the saturation magnetization of the ferrofluid, with an operating point in the linear magnetization regime. For the case of a nonmagnetic top reflective layer, the surface deformation is predicted to be (liquid thickness/(4f#)), where f# is the f-number of the LM. For example, for a mirror with f# of 5 and liquid thickness of 1 mm, the surface deformation under tilting condition is predicted to be 50 μm.

3.4 Honeywell Code base

The Honeywell code base and documentation developed by the Honeywell team[32] contains two M&S documentation files and the computer code bases.

The file "_DARPA_Zenith__Software_v0_Report" contains documentation on modeling relating the ferrofluid surface profile to the magnetic field conditions and device design. The file "Zenith_M&S_Report_v0" documents the Optical model, is tied to the 2D analytical model for ferrofluid deformation.

In the "_DARPA_Zenith__Software_v0_Report", the Kelvin body force expression is derived for the ferrofluid in equilibrium in presence of a magnetic field. Considering gravity and magnetic force, momentum conservation equation is derived for the ferrofluid interface. The magnetic field is calculated using Maxwell equations.

Making further assumptions such as the use of low density ferrofluid for which magnetic susceptibility <<1 and the surface tension force is comparatively small, it was shown[32] that the ferrofluid interface is determined by the equipotential lines (considering magnetic and gravity forces).

The next task is to determine the equipotential lines for any specific Halbach array configuration. The unit cell of a Halbach array is a set of four magnets rotated with respect to one other. The unit cell can be repeated indefinitely. This configuration gives rise to a flat magnetic field on one side and nearly zero magnetic field on the opposite side. An analytical expression for the magnetic field has been derived and implemented in Matlab. The magnetic field is linear with magnetization and decreases exponentially from the top surface of the Halbach array. An analytical expression for the ferrofluid surface amplitude and the total body force potential were derived. The body force potential gives the ferrofluid surface profile assuming it follows the equipotential line. The analysis was extended to derive an expression for the critical magnetization field for the onset of Rosensweig instability, which forms a serrated surface pattern. This analytical framework is the basis for the code bases described below.

The analytical expression for the ferrofluid surface amplitude was solved using Matlab to produce the mid-frequency wavefront error as a function of saturation magnetization and magnet height/wavelength ratio. This includes assumptions such as absence of edge effects, saturation magnetization much less than the magnetic field strength and the use of a commercial ferrofluid. Several plots relating various design factors help in determining the optimum operating conditions in terms of saturation magnetization, ferrofluid height and magnet spacing.

The Halbach array code generates the magnetic flux density and Kelvin body force for a 2D flat Halbach array. The spherical global tilting code produces the equipotential fluid surface for a 2D spherical Halbach array, assuming an ideal Mallinson[32] magnetic field. The equipotential surface is calculated as a function of tilt angle, which was then used in the optical code.

The analytical model cannot be used for a curved Halbach array with discrete magnets. A more accurate 3D COMSOL model was developed for the curved liquid mirror.

The documentation file "Zenith_M&S_Report_v0" contains information on the calculation of optical performance of the liquid mirror of this design. The input to the model is the result of the Matlab 2D spherical global tilting code described above. The 2D results can be analyzed using a 3D Zernike fitting process. The input to the model is the height profile of the ferrofluid surface as a function of tilt. Tip/tilt and curvature are first removed to see the mid-frequency ripple due to the Halbach array. The mid-frequency ripple was found to be independent of the tilt angle. Assuming the ripple can be corrected to 1% residual level using shims, simulated shim-corrected curves can then be generated.

In the optical model, the piston, tilt and curvature are first removed from the equipotential surface obtained from the 2D spherical global tilting code. This gives the global wavefront error. The rest of the code carries out "what if" analyses to determine what is ideally possible. The code calculates residual wavefront error versus radial location as a function of tilt after numerically fitting and removing coma and spherical aberration terms. The residual error is the uncorrected mid-frequency error. The code then can carry out another "what if" exercise to remove periodic error in the residual wavefront to yield 10 nm rms residual error, and the associated point-spread function.

The baseline design assumption is that the 99% of the mid-frequency errors can be corrected by magnetic shims.

These code bases for tiltable liquid mirror telescopes are being made publicly available. The code bases are hosted on Github and Box, and may be obtained at no cost until December 2025 by sending an email request to zenith@darpa.mil.

4. SUMMARY

The Zenith program is investigating four approaches to developing half-meter and larger scale liquid mirror telescopes. The liquid mirror in three of these approaches is based on a ferrofluid combined with a MELLF, and a fourth approach employs liquid Mercury as the mirror material. Since the telescope must be able to tilt and track and slew while imaging, spin-stabilization is excluded. This has led to the design and implementation of other, new means of controlling a diffraction-limited imaging-quality mirror surface, i.e., by using a combination of magnetic, electrostatic and capillary means. The sloshing behavior of liquids when the mirror is in motion is being addressed through viscosity control and use of porous media. The absence of centrifugal forces also requires the development of new substrate material surfaces/coatings that statically ensure wetting and adhesion. New formulations of ferrofluids, MELLFs and optional protective coatings for MELLF are being actively developed. The processes for repeatable formation of the liquid system, application of the MELLF layer and replenishment of the liquid system during long term operation are also in development. The objective is to enable next-generation LMs and LMTs that are tiltable and have an optical quality imaging surface that can be maintained for long periods without defects or instabilities.

Alongside the development of successful recipes for 50-cm-scale non-rotating LMs, development of custom control systems required to maintain high-quality imaging capability at rest and during tilt and slew are in progress. The non-alignment of gravity and the optical axis during tilt results in non-uniform surface wavefront error distribution. The liquid sub-system, the shape and surface control sub-system (magnetic or capillary or electrostatic or some combination thereof), in-situ mirror metrology sub-system (interferometry, deflectometry, etc.), along with real-time closed-loop adaptive optic control of the WFE of the mirror must all be integrated into an operational LMT system.

The Zenith program is addressing these challenges. A set of openly available M&S tools have been developed to enable future development of large-diameter liquid mirror telescopes. The modelling and simulation tools (tiltable liquid mirror codes) are available on request to zenith@darpa.mil, until December 2025.

ACKNOWLEDGMENTS

All work described in this paper was funded by the Defense Advanced Research Projects Agency (DARPA) Defense Sciences Office (DSO). The Mercury Liquid Mirror Based on Electrowetting-on-Dielectric (EWOD) Approach was funded by contract number FA237724CB009. The Capillary-Assisted and Magnetically Controlled Ferrofluidic Approach was funded by contract number FA237724CB010. The Magnetically Controlled Ferrofluidic with a Porous Wicking Structure Approach was funded by contract number FA237724CB008. The Magnetically Controlled Self-Assembling Ferrofluidic Ionic Bilayer Liquid Approach was funded by contract number FA237724CB011.

Additionally, Michael Nayak would like to acknowledge the support of Lee Pele and Dr. Matthew Julian in the ideation, construction and execution of the DARPA Zenith program. This paper has been approved for public release (reference number 39855).

CODE AND DATA AVAILABILITY

All data in support of the findings of this paper are available within the article or as supplementary material.

REFERENCES

[1] https://science.nasa.gov/mission/hubble/
[2] https://webbtelescope.org/news/webb-science-writers-guide/telescope-overview
[3] Cole, G., "James Webb Telescope Mirror Polishing," Princeton Plasma Physics Laboratory presentation, 13 September 2023, https://www.pppl.gov/events/2023/james-webb-telescope-mirror-polishing
[4] J. Foust, "Envisioning the next generation of space telescopes", https://spacenews.com/envisioning-the-next-generation-of-space-telescopes/
[5] Drummond, J. D. and Rast, R. H., "First Resolved Images of a Spacecraft in Geostationary Orbit with the Keck-II 10 m Telescope," 2010 Advanced Maui Optical and Space Surveillance Technologies Conference, 14-17 Sep, Maui, HI.
[6] Plait, P., "Sentinel-1A Satellite Slammed by Space Debris," Slate, 30 September 2016, https://slate.com/technology/2016/09/sentinel-1a-spacecraft-was-hit-by-space-debris.html.
[7] Bruce Murray Space Image Library, "Teeny impact on the OSIRIS-REx sample return capsule heat shield," 02 March 2017, https://www.planetary.org/space-images/teeny-impact-on-the.
[8] Iyer, K. A., Mehoke, D. S., Chadegani, A. and Batra, R. C., " Glass surface spall size resulting from interplanetary dust impacts," IEEE Aerospace Conference, Big Sky, MT, USA, 2015, pp. 1-9, doi: 10.1109/AERO.2015.7119067 (2015).
[9] NASA Orbital Debris Program Office, https://orbitaldebris.jsc.nasa.gov/modeling/legend.html.
[10] Gough, E., "How can we bring down the costs of large space telescopes?," Phys.Org, 15 September 2023, https://phys.org/news/2023-09-large-space-telescopes.html.
[11] Alpai, D., "Future Space Telescopes Could Return to Old Lens Technology to Save Costs," Sciencealert.com, 13 July 2023, https://www.sciencealert.com/future-space-telescopes-could-return-to-old-lens-technology-to-save-costs.
[12] Wang, B., "Fluidic Telescopes Could Breakthrough Cost Limits to 50 Meter Space Telescopes," nextbigfuture.com, 23 January 2023, https://www.nextbigfuture.com/2023/01/fluidic-telescopes-could-breakthrough-cost-limits-to-50-meter-space-telescopes.html.

[13] https://www.nasa.gov/science-research/astrophysics/what-is-the-fluidic-telescope/.
[14] Cabanac, R. A., Borra, E. F. and Beauchemin, M., “A Search for Peculiar Objects with the NASA Orbital Debris Observatory 3 Meter Liquid Mirror Telescope,” Astrophys. J. 509, 309–323 (1998).
[15] Brousseau, D., Borra, E. F., Jean-Ruel, H., Parent, J. & Ritcey, A, “A magnetic liquid deformable mirror for high stroke and low order axially symmetrical aberrations,” Opt. Express 14, 11486 (2006).
[16] https://www.astronomy.com/science/unique-liquid-mirror-telescope-comes-online-in-india/
[17] Stahl, H.P. and Allison, M., “Parametric cost model for ground and space telescopes”, SPIE Proceedings 11450, Modeling, Systems Engineering, and Project Management for Astronomy IX (2020).
[18] Laird, P. R., Borra, E. F., Bergamasco, R., Gingras, J., Truong, L. and Ritcey, A., “Deformable mirrors based on magnetic liquids,” Proc. SPIE 5490, Advancements in Adaptive Optics, https://doi.org/10.1117/12.552141 (2004).
[19] Brousseau, D., Borra, E. F., Rochette, M. and Landry, D., B., “Linearization of the response of a 91-actuator magnetic liquid deformable mirror,” Opt. Express 18, 8239-8250 (2010).
[20] Surdej, J., Ailawadhi, B., Akhunov, T., Borra, E., Dubey, M., Dukiya, N., Fu, J., Grewal, B., Hickson, P., Kumar, B., Misra, K., Negi, V., Pospieszalska-Surdej, A., Pranshu, K. and Sun, E., “The 4m International Liquid Mirror Telescope: a brief history and some preliminary scientific results,” arXiv:2311.05623 [astro-ph.IM], https://doi.org/10.48550/arXiv.2311.05623 (2023).
[21] Wang, W., Timonen, J.V.I., Carlson, A. et al., “Multifunctional ferrofluid-infused surfaces with reconfigurable multiscale topography,” Nature 559, 77–82, https://doi.org/10.1038/s41586-018-0250-8 (2018).
[22] Caillosse, E., Zaier, M., Mezghani, M., Hajjar-Garreau, S., Vidal, L., Lougnot, D. and Balan, L., “Photo-Induced Self-Assembly of Silver Nanoparticles for Rapid Generation of First and Second Surface Mirrors,” ACS Applied Nano Materials, 3 (7), 6531-6540 DOI: 10.1021/acsanm.0c01010 (2020).
[23] Khan, M., R., Eaker, C., B., Bowden, E. F. and Dickey, M. D., “Giant and switchable surface activity of liquid metal via surface oxidation,” 111 (39) 14047-14051, https://doi.org/10.1073/pnas.1412227111 (2014).
[24] Eaker, C. B. and Dickey, M. D., “Liquid metal actuation by electrical control of interfacial tension,” Appl. Phys. Rev., 3 (3): 031103. https://doi.org/10.1063/1.4959898 (2016).
[25] Ren, H., Fox, D., Anderson, P. A., Wu, B. and Wu, S., “Tunable-focus liquid lens controlled using a servo motor,” Opt. Express 14, 8031-8036 (2006).
[26] Li, H., Ren, W., Yang, L., Ma, C., Tang, S. and Yuan, R. “Tunable-focus liquid lens actuated by a novel piezoelectric motor,” Proc. Inst. of Mechanical Engineers, Part C: Journal of Mechanical Engineering Science. 235(19):4337-4347. doi:10.1177/0954406220971666 (2021).
[27] https://www.corning.com/worldwide/en/products/advanced-optics/product-materials/corning-varioptic-lenses.html.
[28] Nayak, M., Basu, S and Iyer, K., “Zenith: A DARPA Liquid Mirror Technology Development Program,” Proc. SPIE 12893, Photonic Instrumentation Engineering XI, 1289305 (11 March 2024); https://doi.org/10.1117/12.2693008.
[29] Mariappan, D., Brousseau, D., Radighieri, G., Kalidoss, S., Shin, D., Thibault, S., Sehgal, H., Abdulkadir, H. and Karnati, S., “Modeling and simulation of Capillary-Operated Space Mesoporous Optical System (COSMOS),” paper 13094-134, SPIE Telescopes + Instrumentation, Yokohama, Japan (2024).
[30] Andersen, T., Choi, H., Gregoriev, R., Kadala, K., Kim, D., Li, Y. and Tarkenton, G., “Design and feasibility study of a scalable liquid mirror,” paper 13100-281, SPIE Telescopes + Instrumentation, Yokohama, Japan (2024).
[31] Hisakado, T., Schroeder, P., Vollmer, D., Dautt-Silva, A., Buczek, S., Shallcross, C., Cabell-Kluch, T., Laut, A., Monton, C., Saumur, M. and Watson, A., “Concept design of an electrostatic actuated controlled liquid mirror,” paper Paper 13094-135, SPIE Telescopes + Instrumentation, Yokohama, Japan (2024).
[32] Rowlands, N., Romero-Calvo, A., Strafford, D., Kamire, R., Childers, A., Yates, S., Rahislic, W., Zheng, S-H., Cameron, P., Cano-Gomez, G., Chen, H., Hu, T., Comstock, E. and Herrada, M., “Development of a self-assembling ferrofluidic ionic liquid mirror“, paper 13100-287, SPIE Telescopes + Instrumentation, Yokohama, Japan (2024).
[33] R. E. Rosensweig, “Ferrohydrodynamics” (Dover, 1997).